



Article

IFPTML Mapping of Drug Graphs with Protein and Chromosome Structural Networks vs. Pre-Clinical Assay Information for Discovery of Antimalarial Compounds

Viviana Quevedo-Tumailli ^{1,2} , Bernabe Ortega-Tenezaca ^{1,3} and Humberto González-Díaz ^{4,5,6,*}

¹ Grupo RNASA-IMEDIR, Department of Computer Science, University of A Coruña, 15071 A Coruña, Spain; viviana.quevedo@udc.es (V.Q.-T.); bernabe.ortega@udc.es (B.O.-T.)

² Research Department, Puyo Campus, Universidad Estatal Amazónica, Puyo 160150, Ecuador

³ Information and Communications Technology Management Department, Puyo Campus, Universidad Estatal Amazónica, Puyo 160150, Ecuador

⁴ Department of Organic and Inorganic Chemistry, University of the Basque Country UPV/EHU, 48940 Leioa, Spain

⁵ BIOFISIKA, Basque Centre for Biophysics, CSIC-UPV/EHU, 48940 Leioa, Spain

⁶ IKERBASQUE, Basque Foundation for Science, 48011 Bilbao, Spain

* Correspondence: humberto.gonzalezdiaz@ehu.es; Tel.: +34-94-601-3547

Abstract: The parasite species of genus *Plasmodium* causes Malaria, which remains a major global health problem due to parasite resistance to available Antimalarial drugs and increasing treatment costs. Consequently, computational prediction of new Antimalarial compounds with novel targets in the proteome of *Plasmodium* sp. is a very important goal for the pharmaceutical industry. We can expect that the success of the pre-clinical assay depends on the conditions of assay per se, the chemical structure of the drug, the structure of the target protein to be targeted, as well as on factors governing the expression of this protein in the proteome such as genes (Deoxyribonucleic acid, DNA) sequence and/or chromosomes structure. However, there are no reports of computational models that consider all these factors simultaneously. Some of the difficulties for this kind of analysis are the dispersion of data in different datasets, the high heterogeneity of data, etc. In this work, we analyzed three databases ChEMBL (Chemical database of the European Molecular Biology Laboratory), UniProt (Universal Protein Resource), and NCBI-GDV (National Center for Biotechnology Information—Genome Data Viewer) to achieve this goal. The ChEMBL dataset contains outcomes for 17,758 unique assays of potential Antimalarial compounds including numeric descriptors (variables) for the structure of compounds as well as a huge amount of information about the conditions of assays. The NCBI-GDV and UniProt datasets include the sequence of genes, proteins, and their functions. In addition, we also created two partitions ($c_{\text{assay}j} = c_{aj}$ and $c_{\text{data}j} = c_{dj}$) of categorical variables from the ChEMBL dataset. These partitions contain variables that encode information about experimental conditions of preclinical assays (c_{aj}) or about the nature and quality of data (c_{dj}). These categorical variables include information about 22 parameters of biological activity (c_{a0}), 28 target proteins (c_{a1}), and 9 organisms of assay (c_{a2}), etc. We also created another partition ($c_{\text{prot}j} = c_{pj}$) including categorical variables with biological information about the target proteins, genes, and chromosomes. These variables cover 32 genes (c_{p0}), 10 chromosomes (c_{p1}), gene orientation (c_{p2}), and 31 protein functions (c_{p3}). We used a Perturbation-Theory Machine Learning Information Fusion (IFPTML) algorithm to map all this information (from three databases) into and train a predictive model. Shannon's entropy measure Sh_k (numerical variables) was used to quantify the information about the structure of drugs, protein sequences, gene sequences, and chromosomes in the same information scale. Perturbation Theory Operators (PTOs) with the form of Moving Average (MA) operators have been used to quantify perturbations (deviations) in the structural variables with respect to their expected values for different subsets (partitions) of categorical variables. We obtained three IFPTML models using General Discriminant Analysis (GDA), Classification Tree with Univariate Splits (CTUS), and Classification Tree with Linear Combinations (CTLC). The IFPTML-CTLC presented the better performance with Sensitivity $Sn(\%) = 83.6/85.1$, and Specificity $Sp(\%) = 89.8/89.7$ for training/validation sets, respectively. This model could become



Citation: Quevedo-Tumailli, V.; Ortega-Tenezaca, B.; González-Díaz, H. IFPTML Mapping of Drug Graphs with Protein and Chromosome Structural Networks vs. Pre-Clinical Assay Information for Discovery of Antimalarial Compounds. *Int. J. Mol. Sci.* **2021**, *22*, 13066. <https://doi.org/10.3390/ijms222313066>

Academic Editor: Aglaia Pappa

Received: 18 October 2021

Accepted: 24 November 2021

Published: 2 December 2021

Publisher's Note: MDPI stays neutral with regard to jurisdictional claims in published maps and institutional affiliations.



Copyright: © 2021 by the authors. Licensee MDPI, Basel, Switzerland. This article is an open access article distributed under the terms and conditions of the Creative Commons Attribution (CC BY) license (<https://creativecommons.org/licenses/by/4.0/>).

a useful tool for the optimization of preclinical assays of new Antimalarial compounds vs. different proteins in the proteome of *Plasmodium*.

Keywords: Antimalarial compounds; *Plasmodium* proteome; NCBI-GDV; UniProt; ChEMBL; machine learning; perturbation theory; complex networks

1. Introduction

Malaria is a major global health concern with cases reported in different regions. At present, the risk areas for contracting this disease are Africa, Central and South America, as well as in some parts of the Caribbean, Asia, Eastern Europe, and the South Pacific. The World Health Organization (WHO) estimated 219 million worldwide reported cases of malaria in 2017. It is an infection of the red blood cells by parasites of the genus *Plasmodium* with the most severe and common forms caused by *Plasmodium falciparum* (*P. falciparum* or *Pf*) and related species such as *Plasmodium vivax* (*P. vivax* or *Pv*), *Plasmodium malariae* (*P. malariae* or *Pm*), and *Plasmodium ovale* (*P. ovale* or *Po*). The most frequent and deadly form is the *Pf*. According to WHO, malaria during pregnancy may cause severe complications. Emerging parasite resistance to available Antimalarial drugs poses great challenges to treatment. Moreover, the costs have significantly increased in the last few years for the determination and development of the new drug. Tufts Center for the Study of Drug Development estimates an out-of-pocket cost per approved drug in \$1861 million for Antimalarial drugs [1–4].

The ChEMBL database lists >17,750 preclinical assays of Antimalarial compounds. The ChEMBL database about Antimalarial compounds cover multiple biological activity parameters (Inhibition, IC₅₀, Activity, etc.), different unique assays only for the protein target of *Pf* organism and is applied to different genes about proteome. In addition, the ChEMBL database compiles datasets of very heterogeneous preclinical assays. We can enrich ChEMBL data with NCBI-GDV and UniProt databases data to obtain information about drug target proteins, chromosomes, and genes. For instance, UniProt includes information related to sequence of proteins. Lastly, NCBI-GDV includes information related to the sequence of genes and the structure of chromosome (DNA sequence, gene adjacency, orientation, etc.) This information may be also relevant for the synthesis of proteins with different functions in the *Pf* [5–11].

On the other hand, IFPTML models have been used in medicinal chemistry, proteomics, nanotechnology, etc., for modeling large datasets with Big Data features. IFPTML models combine Information Fusion (IF) techniques with Perturbation Theory (PT) ideas and Machine Learning (ML) algorithms (PT + ML = PTML models). IFPTML modeling is also useful to carry out information fusion of data from diverse sources. For instance, we can include data about the protein sequence from GenBank, Metabolic networks, Nanoparticles, or even information about epidemiology data in USA counties, etc. [12–14].

In order to develop IFPTML models, we need to use as input variable parameters able to quantify the information about the structural and experimental conditions of assay of all the systems involved (drugs, proteins, gene networks, etc.). In this sense, Shannon's Entropy information measures introduced by Claude E. Shannon could be extremely useful [15]. In fact, Graham, Marrero-Ponce, Barigye, and other researchers, have used different classes of Shannon information values to measure chemical and/or biologically relevant information quantitatively [16–27]. González-Díaz and Munteanu combined the idea of Shannon entropy with Markov chains to calculate the $Sh(syst)_k$ values, stochastic Shannon's Entropies of order k^{th} , and different molecular systems [28].

In previous work, we analyzed the proteome/genome and chromosomes of *Pf* using data from NCBI-GDV and UniProt databases [29]. However, this previous work has not considered the possibility of mapping this data vs. preclinical assays of compounds towards the design of new Antimalarials. In addition, there are no reports IFPTML models for

Antimalarial compounds considering information from NCBI-GDV, UniProt, and ChEMBL databases at the same time. In this work, we develop a general-purpose IFPTML model for the prediction of new Antimalarial compounds by fusing information from the three different databases. Figure 1 illustrates all the different steps that are included in the general workflow used to obtain this IFPTML model. Firstly, we downloaded all relevant information from the ChEMBL, NCBI-DVG, and UniProt databases. These three datasets were merged into one using IF techniques. This new dataset was cleaned and pre-processed by applying several criteria, e.g., eliminating preclinical assays that do not register values in biological activities. Next, we calculated the $Sh(syst)_k$ of the different sub-systems involved, such as, drugs, protein sequences, genes and chromosomes using Markov Chains models. After that, PTOs with the form of MAs were used to quantify deviations in the structural parameters $Sh(syst)_k$ (numerical parameters) concerning changes in the experimental conditions (categorical variables). This allowed us to quantify it in simple PTOs information from the structure and experimental conditions of assays of all the sub-systems involved. Finally, we trained, validated, and compared the IFPTML models. The role of the different sources of information was discussed as well. This kind of analysis opens a new way to carry IF combined with ML modeling towards discovering new antimalarial compounds using preclinical assays and proteome information.

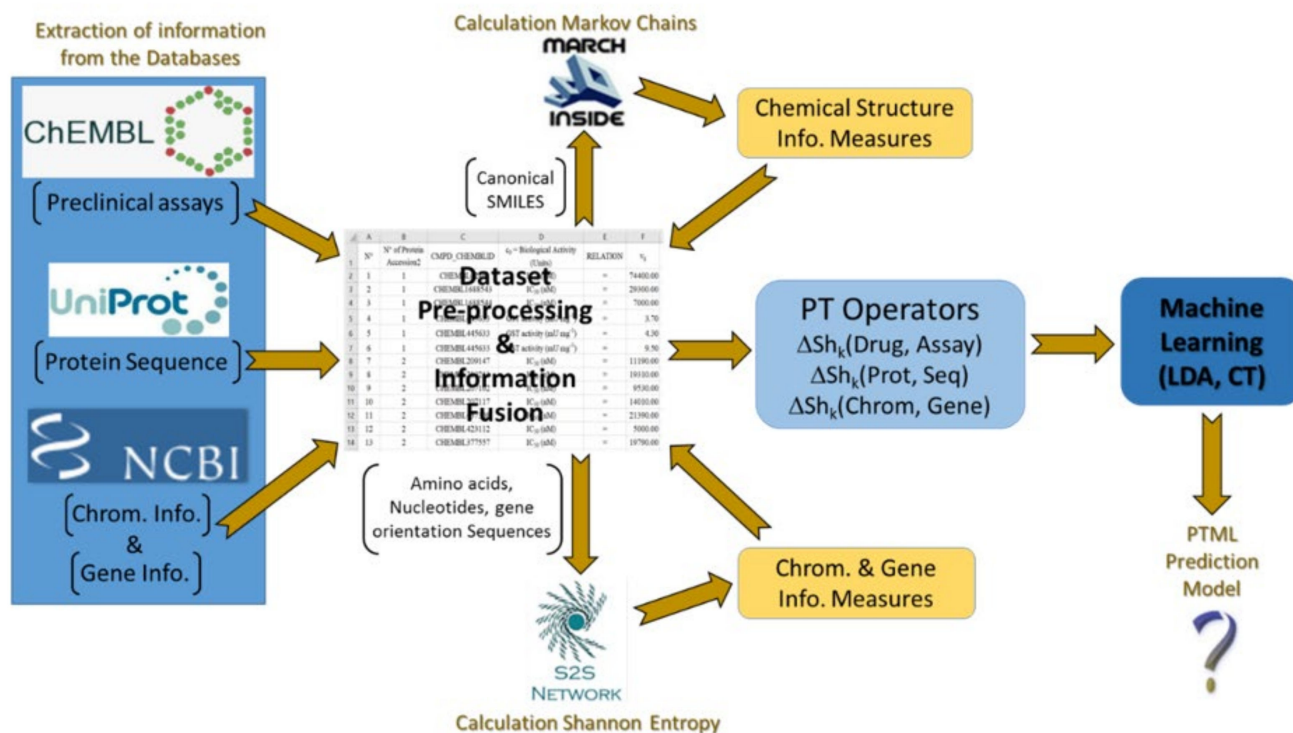


Figure 1. General Workflow of the steps given in this work.

2. Results

We developed various IFPTML models using PTOs and the MMAs operators [14]. The model calculated the scoring function $f(v_{ij})_{calc}$ for outcome of i^{th} drug vs. j^{th} protein in preclinical assay multiple conditions of assay defined by the categorical variables c_j . The first model developed was the IFPTML-GDA linear model. The Equation (1) of this model is the following:

$$\begin{aligned}
 f(v_{ij})_{\text{calc}} = & -20.12298 + 99.13885 \cdot f(v_{ij})_{\text{ref}} \\
 & + 0.74880 \cdot \Delta\text{Sh}(\text{Drug}; \text{Csat})_{5c_{aj}} \\
 & - 2.20919 \cdot \Delta\text{Sh}(\text{Drug}; \text{Hetero})_{5c_{aj}} \\
 & + 3.36764 \cdot \Delta\text{Sh}(\text{Drug}; \text{Hx})_{1c_{aj}} \\
 & + 2.39122 \cdot \Delta\text{Sh}(\text{Drug}; \text{Csat})_{1c_{pj}} \\
 & + 2.25745 \cdot \Delta\text{Sh}(\text{Drug}; \text{Hetero})_{4c_{pj}} \\
 & - 3.32408 \cdot \Delta\text{Sh}(\text{Drug}; \text{Hx})_{4c_{pj}} \\
 & - 2.88041 \cdot \Delta\text{Sh}(\text{Drug}; \text{Csat})_{1c_{dj}} \\
 & + 6.57931 \cdot \Delta\text{Sh}(\text{Drug}; \text{Halog})_{1c_{dj}} \\
 & - 6.84622 \cdot \Delta\text{Sh}(\text{Drug}; \text{Halog})_{2c_{dj}} \\
 & - 0.00877 \cdot \Delta\text{Sh}(\text{Chr}; \text{Gen})_{5c_{aj}} \\
 & + 0.46021 \cdot \Delta\text{Sh}(\text{Prot}; \text{Seq})_{5c_{dj}}
 \end{aligned} \tag{1}$$

$$n = 17758\chi^2 = 6595.853 \quad p < 0.05$$

The variables in this IFPTML model result from several procedures of pre-processing and post-processing (after obtaining the model) of the input/output variables. For instance, the output of the model is the scoring function $f(v_{ij})_{\text{calc}}$. This is a real value function useful to quantify the possibilities with which the i^{th} drug gives a positive outcome in the j^{th} with preclinical assay with categorical variables $c_j = c_{aj}, c_{pj}$ and c_{dj} (experimental conditions, etc.).

In Figure 2, we give details of the procedures carried out for pre-processing and post-processing of the variables. After the post-processing procedure, we were able to compare inputs vs. outputs of the IFPTML model in order to obtain the classification matrix and measure its performance.

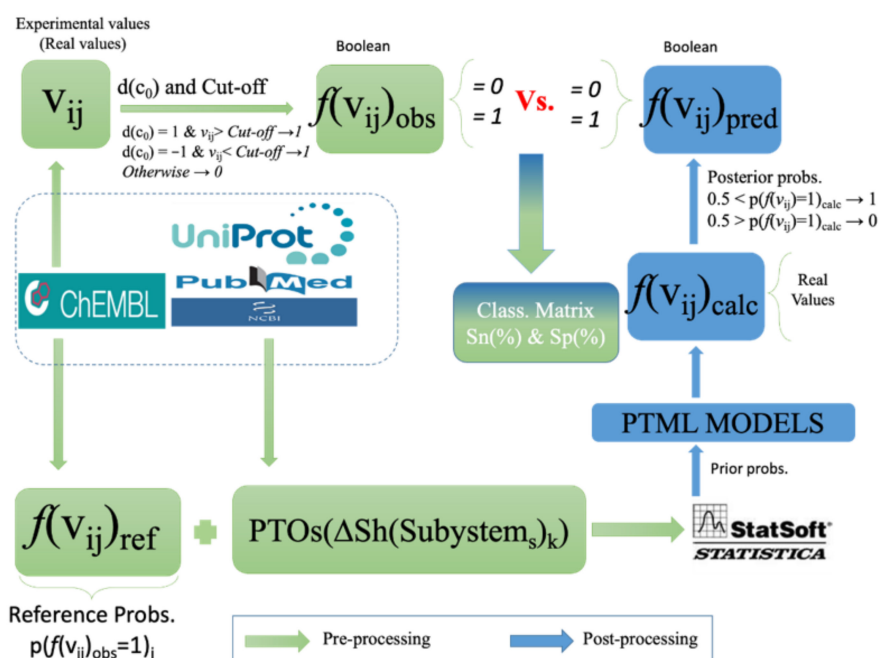


Figure 2. Variables pre-processing vs. post-processing.

In addition in Table 1, we can see that the model is unbalanced with high values of Sp(%) and Accuracy Ac(%) > 98 in training and validation, but the values of Sn(%) are low. The other statistical parameters of the model are as follows: n is the number of cases used to train the model equal to 17,758; χ^2 is the Chi-square statistics equal to 6595.853; and p is the p-level with a value less than 0.05. Multiple input variable encoding information related to

the structure and conditions of assay of the drug is entered into the model using a forward stepwise feature selection strategy [30]. The model also includes variables encoding information about the protein sequence, gene sequence, and chromosome structure such as $\Delta\text{Sh}(\text{Prot}; \text{Seq})_{5\text{cdj}}$ and $\Delta\text{Sh}(\text{Chr}; \text{Gen})_{5\text{caj}}$. However, they seem to have a lower contribution.

Table 1. IFPTML-GDA model result.

Observed Sets ^a	Statistical Parameter ^b	Predicted		Predicted Sets	
		Statistics	n_j	$f(v_{ij})_{\text{pred}} = 0$	$f(v_{ij})_{\text{pred}} = 1$
Training Series					
$f(v_{ij})_{\text{obs}} = 0$	Sp(%)	98.8	13,087	12,934	153
$f(v_{ij})_{\text{obs}} = 1$	Sn(%)	65.9	232	79	153
total	Ac(%)	98.3	13,319		
External Validation Series					
$f(v_{ij})_{\text{obs}} = 0$	Sp(%)	98.7	4365	4310	55
$f(v_{ij})_{\text{obs}} = 1$	Sn(%)	66.2	74	25	49
total	Ac(%)	98.2	4439		

^a The observed classification classes are two: drugs with a desired level of biological effect observed $f(v_{ij})_{\text{obs}} = 1$ or $f(v_{ij})_{\text{obs}} = 0$ otherwise. ^b Sn (%) = Sensitivity, Sp (%) = Specificity and AC (%) = Accuracy.

In the classification matrix, we can see that the number of positive cases $n(f(v_{ij}) = 1)$ obtained after application of the cutoff values is very unbalanced with respect to the number of cases $n(f(v_{ij}) = 0)$ in the control series. In fact, we have $n(f(v_{ij}) = 1) = 232$ in training and 74 in validation vs. $n(f(v_{ij}) = 0) = 13,087$ in training and 4365 in validation for the control group. We carried out a cutoff scanning study to verify whether it could be caused due to a very restrictive value of the cutoffs or not. As can be seen in Table 2, the number of numbers of positive cases $n(f(v_{ij}) = 1)$ do not vary notably and is in all very low cases for all the ranges of cutoff which is interesting for antimicrobial chemotherapy uses. For instance, in the case of Inhibition(%) the $n(f(v_{ij}) = 1) < 230$ for all values of cutoff in the range Inhibition(%) = 75–100. The number of positive cases increases in the range $n(f(v_{ij}) = 1) = 300$ –9700 only for Inhibition(%) < 50%, which is not a clinically useful range. In other properties like IC_{50} (nM) and K_i (nM), the number of positive cases $n(f(v_{ij}) = 1) < 140$, cases in all the cutoff 1–100 nM ranges and for all values of cutoff in the range Inhibition(%) = 75–100. Due to all these problems, we tried to also test non-linear IFPTML models (see next section).

Table 2. Selected values of multi-condition averages for different combinations of assay conditions.

c_0 = Activity (Units)	Cut-off(c_0)								Total
	1	10	25	50	75	95	100	200	
Inhibition (%)	9785	1535	564	376	228	78	39	-	13,469
IC_{50} (nM)	2	29	49	81	101	108	110	133	3715
K_i (nM)	24	78	100	120	132	134	138	160	369
Other Activities	59	133	146	148	150	149	150	152	205
$n(f(v_{ij}) = 1)$	9870	1775	859	725	611	469	437	445	17,758
$n(f(v_{ij}) = 0)$	7888	15,983	16,899	17,033	17,147	17,289	17,321	17,313	

One of the non-linear IFPTML models found was the Classification Tree (CT)—IFPTML model (IFPTML-CTUS), which is a CT model based on a Univariate Splitting (US) rule [30]. In this model, the prior probabilities with which a compound is predicted as active were set at $\pi_1 = 0.5$. These probabilities are perfectly balanced compared with the unbalanced prior probabilities of $\pi_1 = 0.7$ used in the GDA-IFPTML model. In Figure 3, we show the decision tree for the IFPTML-CTUS model.

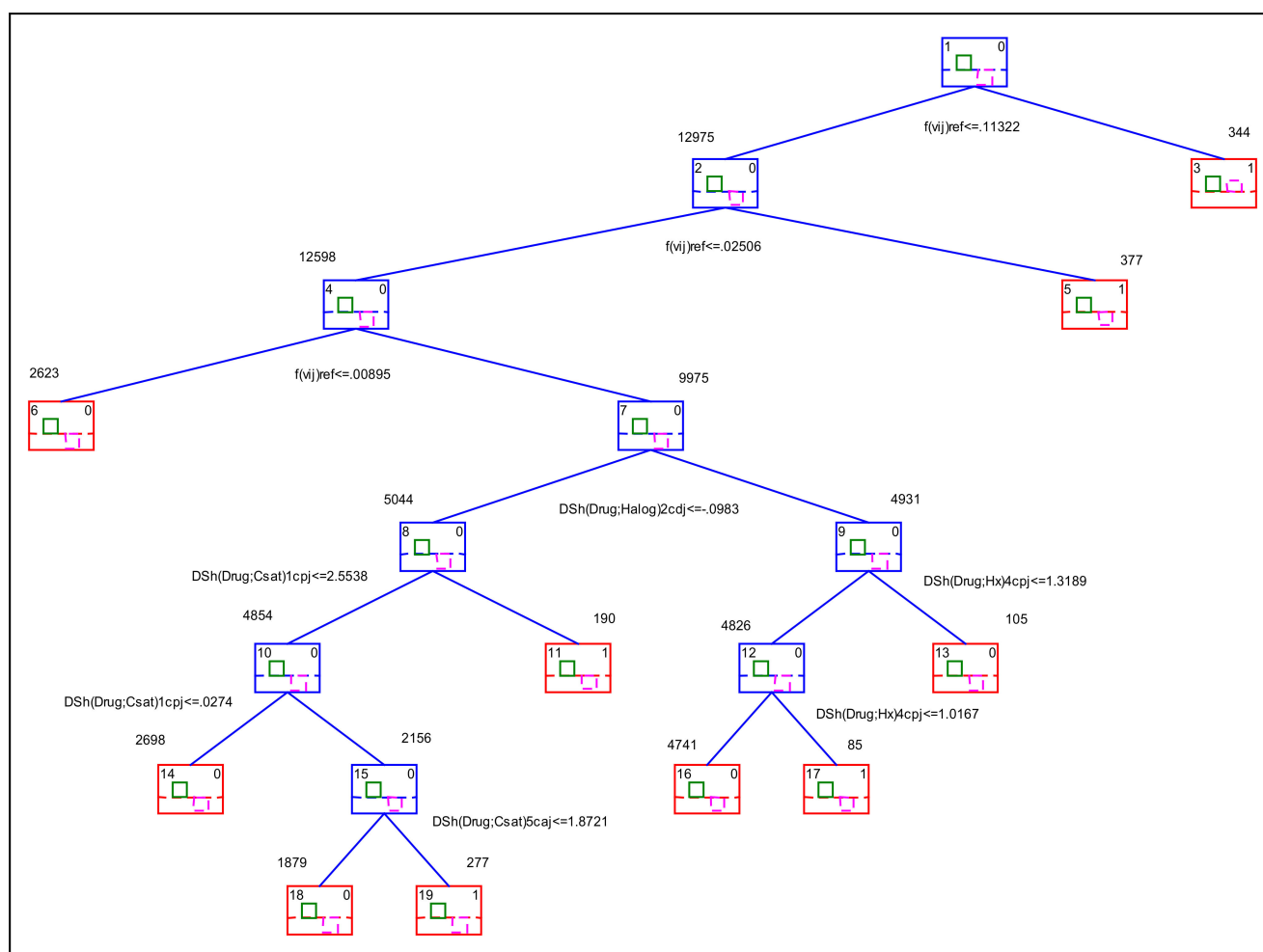


Figure 3. IFPTML-CTUS model decision tree.

In Table 3, we show the results and coefficients of all the variables in the different splitting rules about the classification tree of this model. The variables that were entered into the model are $\Delta Sh_1 = \Delta Sh(\text{Drug};\text{Halog})_2c_{dj}$, $\Delta Sh_2 = \Delta Sh(\text{Drug};\text{Csat})_1c_{pj}$, $\Delta Sh_3 = \Delta Sh(\text{Drug};\text{Hx})_4c_{pj}$, $\Delta Sh_4 = \Delta Sh(\text{Drug};\text{Csat})_1c_{pj}$, $\Delta Sh_5 = \Delta Sh(\text{Drug};\text{Hx})_4c_{pj}$, $\Delta Sh_6 = \Delta Sh(\text{Drug};\text{Csat})_5c_{aj}$.

Another model found was the IFPTML-CTLC, which is a IFPTML model based on CT but using Linear Combinations (LC) as split rules. In Figure 4, we show the decision tree for the IFPTML-CTLC model. In Table 4, we show the coefficients of all the variables in the different LCs used as splitting rules.

In the first instance, we compared the models in terms of performance. In Table 5, we can see a comparison of the three IFPTML models developed in this research: GDA, CTUS, and CTLC. The IFPTML-GDA model showed the lowest value of $Sn(\%) = 65.9/66.2$ and $Sp(\%) = 98.7/98.8$ for training and validation, respectively. Both IFPTML-CT models have balanced prior probabilities $\pi_1 = 0.5$ with which a compound is predicted as active (compared $\pi_0 = 0.5$). These values are perfectly equilibrated, remember that the IFPTML-GDA models presents important unbalance in this regard with $\pi_1 = 0.7$ (compared $\pi_0 = 0.3$). In addition, both IFPTML-CT models achieved values of $Sn(\%)$ and $Sp(\%)$ greater than 80.0%. The values of IFPTML-CTUS are equal to $Sn(\%) = 81.0/82.4$ and $Sp(\%) = 91.7/91.6$. The IFPTML-CTLC also has high values of $Sn(\%) = 83.6/85.1$ and $Sp(\%) = 89.7/89.8$.

Table 3. IFPTML-CTUS model coefficients.

Class	Left	Right	Control	Active	Predict.	Split	Split
Node	Branch	Branch	$n(f(v_{ij}) = 0)$	$n(f(v_{ij}) = 1)$	Class	Constant	Variable
1	2	3	13,087	232	0	0.11321607	$f(v_{ij})_{refi}$
2	4	5	12,903	72	0	0.02505894	$f(v_{ij})_{refi}$
3			184	160	1		–
4	6	7	12,542	56	0	0.00895431	$f(v_{ij})_{refi}$
5			361	16	1		–
6			2623	0	0		–
7	8	9	9919	56	0	–0.0982586	$\Delta Sh(Drug;Halog)_2c_{dj}$
8	10	11	5006	38	0	2.55375728	$\Delta Sh(Drug;Csat)_1c_{pj}$
9	12	13	4913	18	0	1.318866	$\Delta Sh(Drug;Hx)_4c_{pj}$
10	14	15	4821	33	0	0.02739699	$\Delta Sh(Drug;Csat)_1c_{pj}$
11			185	5	1		–
12	16	17	4809	17	0	1.01671015	$\Delta Sh(Drug;Hx)_4c_{pj}$
13			104	1	0		–
14			2681	17	0		–
15	18	19	2140	16	0	1.87205633	$\Delta Sh(Drug;Csat)_5c_{aj}$
16			4726	15	0		–
17			83	2	1		–
18			1868	11	0		–
19			272	5	1		–

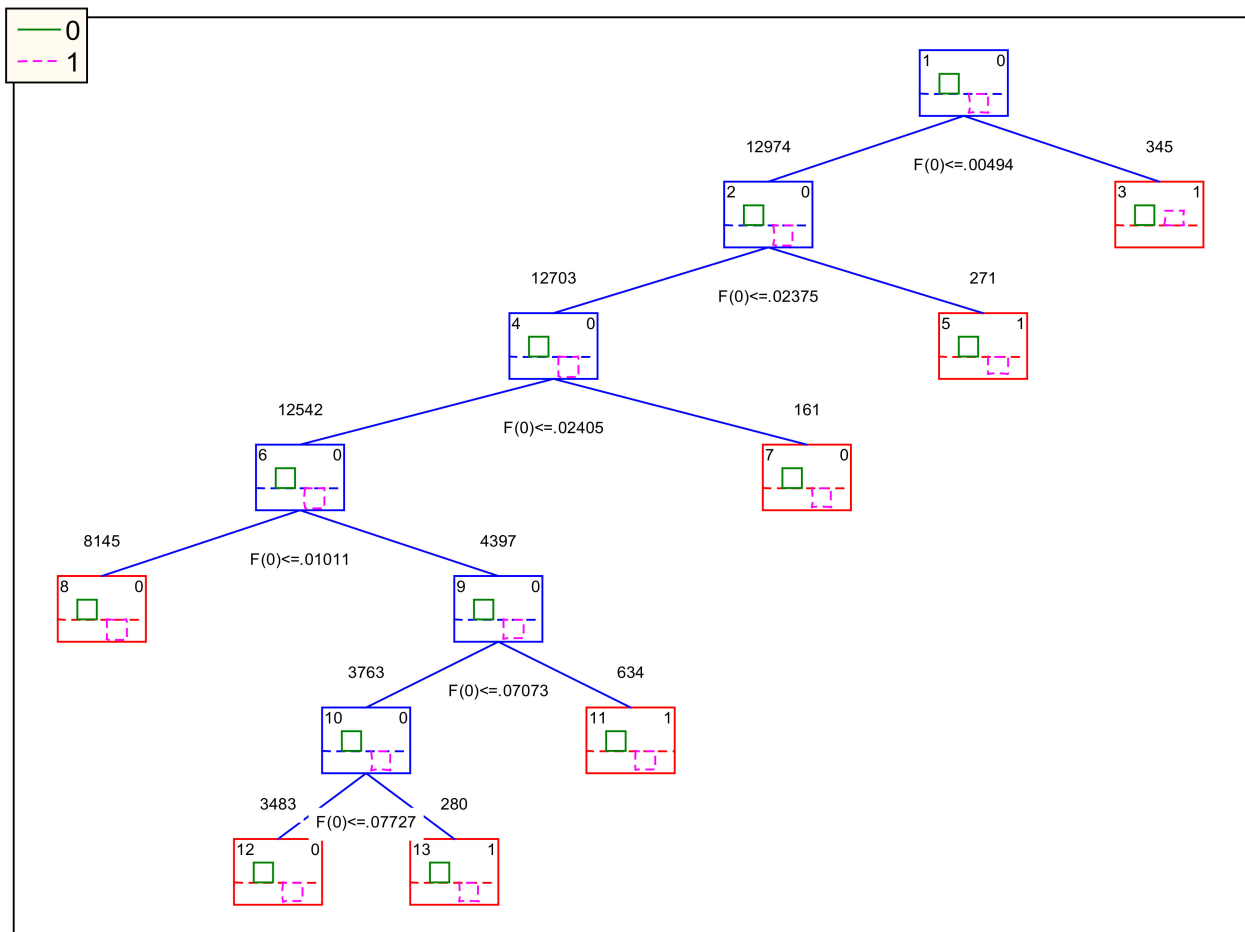


Figure 4. IFPTML-CTLC model decision tree.

Table 4. IFPTML-CTLC model coefficients.

Var	Coeff.	$f(v_{ij})_{01}$	$f(v_{ij})_{02}$	$f(v_{ij})_{03}$	$f(v_{ij})_{04}$	$f(v_{ij})_{05}$	$f(v_{ij})_{06}$	Mean	S.D.
Split const.	a_{00}	−0.005	−0.024	−0.024	−0.010	−0.071	−0.077	−0.04	0.03
$f(v_{ij})_{ref}$	a_{01}	0.044	0.762	0.751	0.818	2.678	2.881	1.32	1.17
$\Delta Sh(\text{Drug};\text{Csat})_5c_{aj}$	a_{02}	0.000	0.008	−0.001	−0.003	−0.008	−0.007	0.00	0.01
$\Delta Sh(\text{Drug};\text{Hetero})_5c_{aj}$	a_{03}	−0.001	−0.010	−0.042	−0.033	−0.103	−0.143	−0.06	0.06
$\Delta Sh(\text{Drug};\text{Hx})_1c_{aj}$	a_{04}	0.001	0.020	0.047	0.047	0.120	0.160	0.07	0.06
$\Delta Sh(\text{Drug};\text{Csat})_1c_{pj}$	a_{05}	0.001	0.014	0.020	0.023	0.083	0.093	0.04	0.04
$\Delta Sh(\text{Drug};\text{Hetero})_4c_{pj}$	a_{06}	0.001	0.009	0.036	0.028	0.078	0.109	0.04	0.04
$\Delta Sh(\text{Drug};\text{Hx})_4c_{pj}$	a_{07}	−0.001	−0.017	−0.038	−0.037	−0.092	−0.117	−0.05	0.04
$\Delta Sh(\text{Drug};\text{Csat})_1c_{dj}$	a_{08}	−0.001	−0.019	−0.016	−0.017	−0.065	−0.079	−0.03	0.03
$\Delta Sh(\text{Drug};\text{Halog})_1c_{dj}$	a_{09}	0.003	0.057	0.087	0.088	0.713	0.577	0.25	0.31
$\Delta Sh(\text{Drug};\text{Halog})_2c_{dj}$	a_{10}	−0.003	−0.059	−0.094	−0.095	−0.740	−0.609	−0.27	0.32
$\Delta Sh(\text{Chr};\text{Gen})_5c_{aj}$	a_{11}	0.000	0.000	0.002	0.002	0.039	0.075	0.02	0.03
$\Delta Sh(\text{Prot};\text{Seq})_5c_{dj}$	a_{12}	0.000	0.004	−0.002	−0.003	0.008	0.024	0.01	0.01

Table 5. Comparison of models with different algorithms.

Algorithm	Set	Class	Stat Param.	Value (%)	$f(v_{ij})_{pred=0}$	$f(v_{ij})_{pred=1}$
IFPTML GDA $\pi_0 = 0.30$ $\pi_1 = 0.70$	Train	$f(v_{ij})_{obs} = 0$	Sp	98.8	12,934	153
		$f(v_{ij})_{obs} = 1$	Sn	65.9	79	153
	Validation	$f(v_{ij})_{obs} = 0$	Sp	98.7	4310	55
		$f(v_{ij})_{obs} = 1$	Sn	66.2	25	49
IFPTML CTUS $\pi_0 = 0.50$ $\pi_1 = 0.50$	Train	$f(v_{ij})_{obs} = 0$	Sp	91.7	12,002	1085
		$f(v_{ij})_{obs} = 1$	Sn	81.0	44	188
	Validation	$f(v_{ij})_{obs} = 0$	Sp	91.6	3997	368
		$f(v_{ij})_{obs} = 1$	Sn	82.4	13	61
IFPTML CTLC $\pi_0 = 0.50$ $\pi_1 = 0.50$	Train	$f(v_{ij})_{obs} = 0$	Sp	89.8	11,751	1336
		$f(v_{ij})_{obs} = 1$	Sn	83.6	38	194
	Validation	$f(v_{ij})_{obs} = 0$	Sp	89.7	3917	448
		$f(v_{ij})_{obs} = 1$	Sn	85.1	11	63

Next, we would like to compare the models in terms of number of input variables, LCs, and number of splitting rules. The IFPTML-GDA uses >10 input variables but only one LC with one splitting rule. Interestingly, the IFPTML-CTUS model uses 5 input variables and 9 splitting constants without relying upon the use of LCs. Conversely, the IFPTML-CTLC is by large the more complicated model of the three with >10 input variables and 6 LCs, each one with its respective splitting constants. For instance, it includes information about the sequence of the protein in the variable $\Delta Sh(\text{Prot};\text{Seq})_5c_{dj}$ and information about the gene and chromosome of this protein with the variable $\Delta Sh(\text{Chr};\text{Gen})_5c_{aj}$. According to these results, we can say that the last model is the best selection in terms of performance and inclusion of biologically relevant information.

Last, we should compare the models regarding the relevance of the biological information included in the input variables. The IFPTML-GDA model contains relevant information about drug structure, protein sequence, etc. By the contrary, the IFPTML-CTUS model does not include information about protein sequence, gene sequence, or chromosome structure. The missing information about the sequence of the protein invalidates the IFPTML-CTUS model for practical uses in the prediction of Antimalarial drugs against a protein target with specific sequence changes (mutations). In fact, mutations in the Malaria gene have been found to be important in the development of drug resistance mechanisms [31,32]. Lastly, the IFPTML-CTLC model includes biological relevant variables related to the target protein, etc., as well as the IFPTML-GDA model. Overall, the IFPTML-CTLC model is the most complex, but at the same time seems to be the more

valuable because it is balanced, has high values of Sn(%) and Sp(%), and includes relevant biological information.

3. Discussion

3.1. IFPTML Linear Model with Multi-Condition Combinatorial Moving Averages (MMAs)

In order to evaluate the performance of the model in terms of Specificity Sp(%) and Sensitivity Sn(%), IFPTML-GDA transforms $f(v_{ij})_{\text{calc}}$ into the Boolean variable $f(v_{ij})_{\text{pred}}$. The variable $f(v_{ij})_{\text{pred}} = 1$ when the compounds are predicted to be active in this assay; $f(v_{ij})_{\text{pred}} = 0$ otherwise. This variable gets the value $f(v_{ij})_{\text{pred}} = 1$ when the posterior probability with the compound is active $p(f(v_{ij}) = 1) \geq 0.5$. The IFPTML-GDA algorithm can estimate the values of posterior probabilities as a sigmoidal function $p(f(v_{ij}) = 1) = \pi_1 / (\pi_1 + \pi_0 \cdot \text{Exp}(-f(v_{ij})_{\text{calc}}))$ of the prior probabilities π_1 and π_0 and the values of the score function. In this model, the prior probabilities with which a compound is predicted as active have been set $\pi_1 = 0.7$ [30]. The deficient number of active compounds in ChEMBL datasets somehow justifies this relatively high value of prior probability, see next discussion.

The main advantage of this IFPTML algorithm is the obtention of a single global model. It means that a unified model has been constructed for preclinical assay optimization of new antimalarial compounds vs. the 28 protein sequences in many different assay conditions c_j . In fact, the model properly predicts the outcome of 17,758 assays in total. This model will also be able to predict new antimalarial compounds for new protein sequences not included in the previous dataset. Otherwise, if we construct one model for each target protein, we will need to train/validate one model for each protein. It means, we need to train/validate a total of 28 individual models, excluding all other variable conditions. Consequently, the IFPTML algorithm can fit one model, performing the job of 28 classic models. In addition, each classic model must be trained with a smaller number of assays. In closing, the models for a single protein are unable to predict the results of one compound for other proteins and/or protein mutants, as they are not sequence sensible.

3.2. IFPTML-CTUS and IFPTML-CTLC Models

The models made the main emphasis on input variables related to chemical information about the structure of the drug and the conditions of assays.

3.3. IFPTML-CTLC Model Practical Use Example

In this section, we illustrate the use of the model with a practical example. We selected the molecule with code ChEMBL264770. See details about this compound in the Supplementary Materials. In Figure 5, we graphically depict all the steps necessary for processing a known or new compound with the present model using ChEMBL264770 as an example. In this figure, we illustrate the three main stages of the algorithm and their more important steps. The IF stage involves steps (1) and (2), the PT stage includes only step (3), and the ML stage includes steps (4) and (5). In step (1), all known information about molecule, target protein, gene, chromosome, and/or assay conditions is downloaded from three databases ChEMBL, UniProt, and NCBI-GDV. In the case of a new compound, the value of biological activity v_{ij} is unknown, but we know all other information about the assay. This information includes numerical variables and categorical variables that encode information on the experimental conditions of the preclinical trials or on the nature and quality of the data. For the molecule ChEMBL264770, the activity parameter is K_i (nM), the UniProt accession ID of target protein is P39898, the assay organism is *Plasmodium falciparum*, the ChEMBL function is Enzyme, the target mapping is a protein, the APD's name and confidence are labeled as ND (Not data), the assay type is B, the curated by Autocur, the number of Confidence Score is 9, and Canonical SMILES. Other data downloaded from NCBI-GDV database are the biological information about target proteins, genes, and chromosomes. Thus, for this example the name of gene in the chromosome XIV is *PF14_0075*, the orientation of gene is 1 which means positive, the protein function is plasmepsin, the nucleotides recurrence of gene and the Genes orientations in this chromosome. All the information downloaded from

these databases was copied into an .xlsx file. In step (2), we calculated the Shannon entropies of the drugs, protein sequences, and chromosome in order to quantify the structural information. For inputs, we used the Canonical SMILES of drugs, the sequence of proteins, sequence of gene, and gene orientation networks (GOIN) of chromosomes. The software MARCH-INSIDE was used to calculate the Shannon information entropy of drugs $Sh(\text{drug})$. Other variables calculated were the Shannon entropies of Amino Acids recurrence $Sh(\text{prot})$, Nucleotides recurrence $Sh(\text{gene})$, and Gene orientation in the chromosome $Sh(\text{Chr})$. These variables were recalculated using the S2SNetwork tool. After step (2) we finished the IF phase and entered the PT phase. In step (3), we calculated PTOs with the form of Moving Average (MA) operators. Up to this point, data cleaning and pre-processing had been performed together with the calculations of the operators applying Perturbation Theory. In step (4), we used the software STATISTICA to run different ML algorithms. For the new molecule, we substituted the values of the operators $\Delta Sh(\text{Drug})_{k,caj}$, $\Delta Sh(\text{Prot})_{k,cpj}$, etc., into these models. Using the IFPTML-GDA model for instance, we can predict an output of $p(f(v_{ij}) = 1) = 0.99$ for this example. This means that the model predicts that this compound is expected to have a value $K_i < 10$ nM (cut-off) with a probability of 0.99. Finally in step (5), we can conclude that the $f(v_{ij})_{\text{pred}} = 1$ (the compound can be considered active according to this assay). As this compound is already known, we can corroborate that this prediction coincides with the observed classification $f(v_{ij})_{\text{obs}} = 1$ which comes from a real value of $K_i = 0.3$ nM. In the case of a compound not previously assayed, one would need to assay the compound in order to corroborate this prediction.

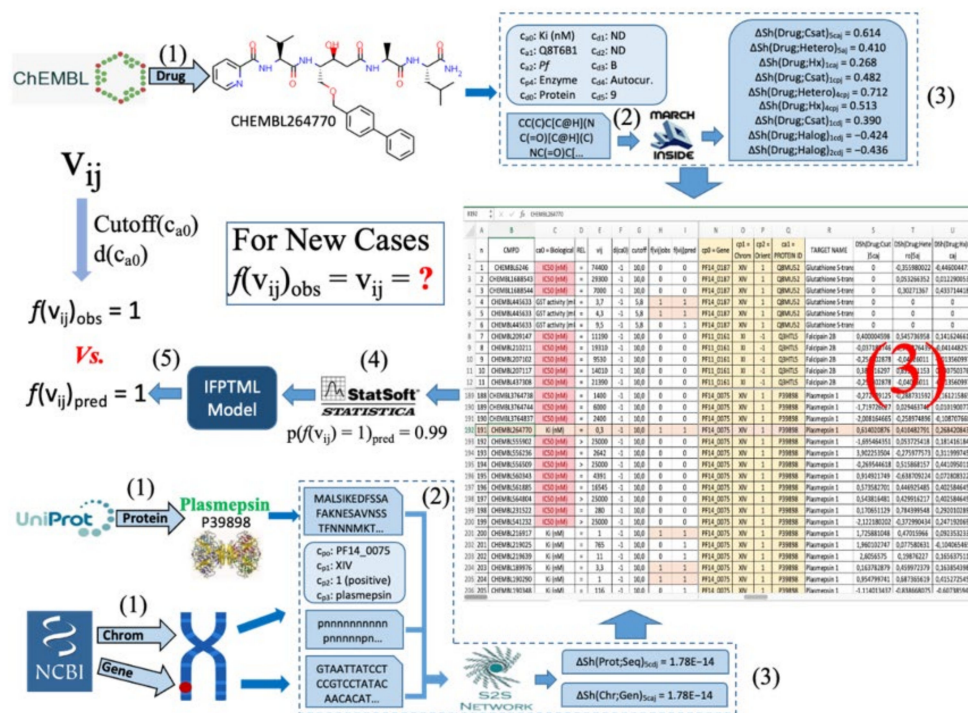


Figure 5. An example of the IFPTML-CTL model.

4. Materials and Methods

4.1. ChEMBL Dataset

We downloaded all the information about proteins and unique assays only for *Pf*. The dataset does not contain another species of intracellular protozoa of the genus *Plasmodium*. The dataset was obtained from the ChEMBL database (<https://www.ebi.ac.uk/chembl/g/#browse/targets> (accessed on 15 November 2018)) using the browser targets tool [33–36]. Initially, the total proteins registered in ChEMBL was 33 for *Pf*. However, the total was 28 proteins, after performing the data pre-processing, which is explained in detail in the next section. The proteins were categorized as follows: 21 Enzymes, 3 Trans-

porters, 1 Epigenetic Regulator, 3 Others Cytosolic Proteins, and 5 Unclassified Proteins. The total number of unique assays outcomes (endpoints) registered for the 33 proteins was 18,381 (statistical cases). Each protein category contains mainly the following fields: ChEMBLID, Preferred Name, UniProt Accession (used to obtain the protein sequences in the UniProt Database), and other fields such as: Target Type, Organism, Compounds, and Endpoints, also called Bioactivities (used to obtain the different assays in the ChEMBL Database). For example, an enzyme ChEMBLID = "CHEMBL1697656" was registered with its Preferred Name = "Glutathione S-transferase", UniProt Accession = "Q8MU52", Target Type = "Single Protein", Organism = "Plasmodium falciparum", Compounds = "4", and Endpoints = "6". Additionally, each endpoint comes from a unique assay with the following main fields: CMPD ChEMBLID, Molecule Name, SMILES, Activity ID, Standard Type, Relation, Standard Value, and Standard Units. Other fields are Assay ID, Assay ChEMBLID, Assay Type, Description, Protein Accession (UniProt Accession), Journal, Year, Volume, and Issue, among others.

4.2. NCBI-GDV Dataset

The *Pf* genome used was originally reported in the Mapviewer database [7,8]. Currently, this dataset is available in the new NCBI-GDV database (<https://www.ncbi.nlm.nih.gov/genome/gdv/> (accessed on 15 November 2017)) [8]. Initially, the *Pf* genome had 14 different chromosomes. Each chromosome contains an average of 383 genes. In this work, we used only 10 out of these 14 chromosomes because the proteins codified by the remnant 4 chromosomes have no biological assays reported in ChEMBL. The genes have a start-and-stop position within the chromosome. The database reports the position (P_{ik}) of each gene in the chromosome and a description of the biological function. The dataset registered the biological sequence of nucleotides of each gene. Additionally, the dataset reports the symbol, the orientation of the gene, as positive or negative ($O_{ik} = 1$ or $O_{ik} = -1$). This information has been found to be somehow relevant to the biological activity of some proteins in *Pf* proteome. Consequently, in this work we also used the Chromosome Gene Orientations Inversion Networks (GOINs) of *Pf* proteome assembled with P_{ik} and O_{ik} information in a previous work [29].

4.3. UniProt Dataset

We downloaded the biological sequence of amino acids of the 28 proteins registered in ChEMBL in FASTA format. The dataset was obtained from UniProt database (<https://www.uniprot.org/> (accessed on 15 November 2018)) using the browser protein tool [9–11]. In turn, the FASTA format has two parameters that were used in this work: string of characteristics and sequence of proteins.

4.4. ChEMBL, NCBI-GDV, and UniProt Information Fusion

We constructed a dataset based on the three previous datasets. In so doing, we carried out an IF process [37–40]. After performing the IF process, the working dataset created contained a total of 18,381 outcomes (rows). We added the canonical SMILE codes and their respective Shannon's Entropy values for each chemical compound. The simplified molecular-input line-entry system (SMILES) codes downloaded from ChEMBL are a notation system used to codify information about the chemical structure of the compounds [41]. SMILES-like representations have been largely used in Cheminformatics [42–47]. We also aggregated the protein sequence and the Shannon's Entropies in each row according to the respective Protein Accession ID. In addition, we added the parameters of each gene and the Shannon's Entropy values for each protein.

4.5. Pre-Processing of the Working Dataset

Firstly, we deleted rows where no values were reported for the variables v_{ij} , PSA, or AlogPin order to clean the dataset. For this reason, the categories of the variable c_{p4} are reduced to 19 Enzymes, 2 Transporters, 1 Epigenetic Regulator, 2 Others Cytosolic Proteins,

and 4 Unclassified Proteins. The total of proteins valid from ChEMBL were 28. Therefore, the data removed represents only a 3.4% of all working dataset. Moreover, all the empty cells of chain type were replaced with the tag ND (No Data). At the end, the dataset to obtain the IFPTML based model had 17,758 rows. In Figure 6, we illustrate the different steps given to pre-processing the data and carrying out the IF process.

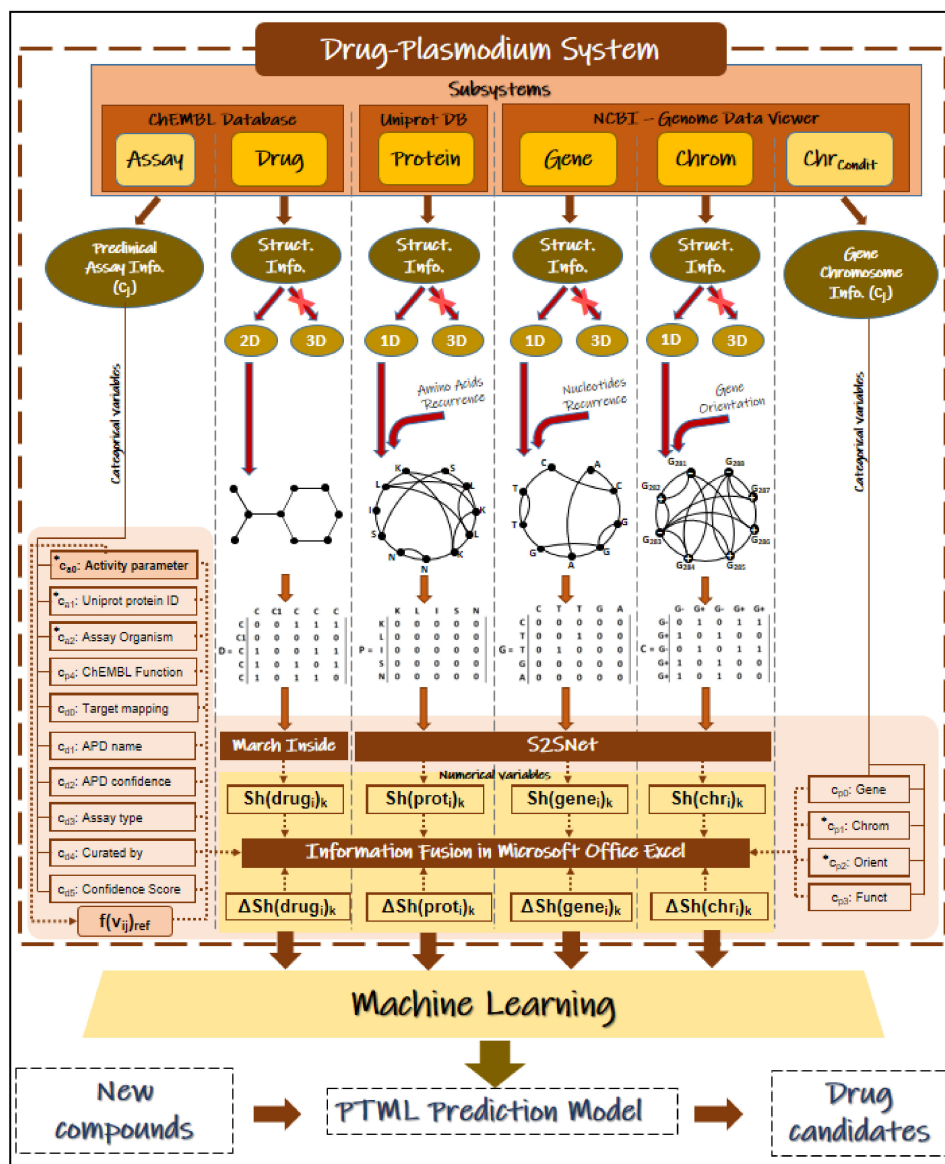


Figure 6. IFPTML model development and IF process.

4.6. IFPTML Shannon Information Theory Models

In Figure 6, we illustrate details of the different steps given to pre-processing the data and train/validate the IFPTML model. First, we performed the IF process, next we calculated the $Sh(\text{Subsystem}_s)_k$ values, the $f(v_{ij})_{ref}$ function values, and the PTOs values (input variables), and then we proceeded to seek the IFPTML models. See more details about the calculation of input/output variables in the next sections. The objective of the IFPTML model is to predict a function $f(v_{ij})_{calc}$ of the observed values $f(v_{ij})_{obs}$. In order to develop the IFPTML model, we took into consideration both structural and functional information for the calculation of the input variables. The structural information refers to the chemical structure of the drug as well as structural features of the target protein, the gene encoding for this target protein, and chromosome of this gene.

We can approach the present problem from the point of view Shannon's Information theory and the theory of Complex Systems. In this sense, we can quantify the relevant structural/functional information of the system with $Sh(\text{Syst})_k$ values calculated using a Markov Chain approach [28]. After that, we calculated the external property of the system $f(v_{ij})_{\text{calc}}$ as a function of a value of reference $f(v_{ij})_{\text{ref}}$ and a function $f(Sh(\text{Syst})_{k,c_j})$ of the structural and functional information. In the Equation (2) we used an IFPTML additive approach to include and separate the different parts of the system or subsystems.

$$f(v_{ij})_{\text{calc}} = a_0 + a_1 \cdot f(v_{ij})_{\text{ref}} + \sum_{s=0, k=0, j=0}^{s_{\text{max}}, k_{\text{max}}, j_{\text{max}}} a_{s,k,j} \cdot \text{PTO} \left[Sh(\text{Subsystem}_s)_{k,c_j} \right] \quad (2)$$

The function of reference $f(v_{ij})_{\text{ref}}$ quantifies the expected value of probability of biological activity for a compound measure under certain experimental conditions specified by the partition c_j of categorical variables. The subsystems considered are $\text{Subsystem}_0 = \text{drug}$, $\text{Subsystem}_1 = \text{protein}$, $\text{Subsystem}_2 = \text{gene}$, and $\text{Subsystem}_3 = \text{chromosome}$. The information about each subsystem will be quantified with the respective Shannon's Entropy information measure values of order k^{th} for each subsystem $Sh(\text{Subsystem}_s)_k$. For instance, $Sh(\text{Subsystem}_0)_k = Sh(\text{Drug})_k$ and $Sh(\text{Subsystem}_1)_k = Sh(\text{Prot})_k$, etc. The value k^{th} can register values from 0 to 5. In addition, the IFPTML model uses PTOs to quantify the deviation (perturbations) in continuous variables (structural parameters, time, concentration, etc.) with respect to functional information encoded by categorical variables c_j (experimental conditions), see details in next sections [14].

In this context, in the Equation (3), we can illustrate the general form of an IFPTML model for the linear cases. In the Equation (4), we selected the linear cases for the sake of simplicity, but in this work, we also reported non-linear models. We can extend the previous equation of the model to write down a general form of the IFPTML model. In so doing, we used MMA as PTOs operators as follows.

$$f(v_{ij})_{\text{calc}} = a_0 + a_1 \cdot f(v_{ij})_{\text{ref}} + \sum_{s=0, k=0, j=0}^{s_{\text{max}}, k_{\text{max}}, j_{\text{max}}} a_{s,k,j} \cdot \Delta Sh(\text{Subsystem}_s)_{k,c_j} \quad (3)$$

$$f(v_{ij})_{\text{calc}} = a_0 + a_1 \cdot f(v_{ij})_{\text{ref}} + \sum_{k=0, j=0}^{k_{\text{max}}, j_{\text{max}}} a_{s,k,j} \cdot \Delta Sh(\text{Drug})_{k,c_j} + \sum_{k=0, j=0}^{k_{\text{max}}, j_{\text{max}}} a_{s,k,j} \cdot \Delta Sh(\text{Prot})_{k,c_j} \\ + \sum_{k=0, j=0}^{k_{\text{max}}, j_{\text{max}}} a_{s,k,j} \cdot \Delta Sh(\text{Gene})_{k,c_j} + \sum_{k=0, j=0}^{k_{\text{max}}, j_{\text{max}}} a_{s,k,j} \cdot \Delta Sh(\text{Chr})_{k,c_j} \quad (4)$$

4.7. Output Variable and Function of Reference

In this work, we developed a IFPTML model for the study of experimental values v_{ij} of biological activity of the i^{th} drug in j^{th} preclinical assays of Antimalarial drugs reported in ChEMBL database. Due to the high number of different biological parameters with different scales and levels of errors, we discretized them to obtain the Boolean function $f(v_{ij})_{\text{obs}}$ to develop a classification model. Firstly, we performed the pre-processing in order to clean the dataset, define/calculate the input, and output variables. Specifically, the $f(v_{ij})_{\text{obs}}$ and $f(v_{ij})_{\text{ref}}$ values have been calculated using excel functions and added to the dataset, see Table 6. For instance, for the calculation of the number of cases with one specific level of c_{a0} (one specific parameter of biological activity) we used the function COUNTIF. The first argument in the syntax is $\text{Range}(c_{a0}) = \text{cells}$ that contain all the values of the categorical variable c_{a0} (names of the parameters of biological activity measured in each preclinical assay). The second argument is $\text{Criteria}(c_{a0}) = \text{cells}$ containing the value of one unique level of c_{a0} (name of one specific parameter of biological activity). The function runs over all $\text{Range}(c_{a0})$ comparing $\text{Criteria}(c_{a0})$ with the specific cell of the $\text{Range}(c_{a0})$. Other arguments used in different functions are $\text{Range}(v_{ij}) = \text{cells}$ that contain all the values of biological activity for all preclinical assays (v_{ij}), $\text{Units}(c_{a0}) = \text{the units of the}$

biological activity measured (c_{a0}), desirability $d(c_{a0}) = 1$ or -1 , and $\text{Range}(f(v_{ij})_{\text{obs}}) = \text{cells}$ that contains the $f(v_{ij})_{\text{obs}}$ value [14].

Table 6. More relevant functions used in the data pre-processing stage.

Variable	Excel Functions Syntax	Notes
$n_j(c_{a0})$	=COUNTIF(Range(c_{a0}), Criteria(c_{a0}))	Function that determines the total number of cases for each Biological activity in the dataset.
$\langle v_{ij}(c_{a0}) \rangle$	=AVERAGEIF (Range(c_{a0}), Criteria(c_{a0}), Range(v_{ij}))	Calculates the average of all the standard values of biological activity in the dataset. It is used as an argument for the cutoff(c_{a0}) function.
cutoff(c_{a0})	=IF(Units(c_{a0}) = %, 95, IF(Units(c_{a0}) = nM, 10, $\langle v_{ij}(c_{a0}) \rangle$)	The cutoff value is used to decide if the compounds is active or not. For the values of Activity(%) and Inhibition(%), the cutoff(c_{a0}) = 95%. Similarly, for the IC ₅₀ (nM), K _i (nM), and K _m (nM), the cutoff(c_{a0}) = 10 nM, etc.
$d(c_{a0})$	=OR($d(c_{a0}) = 1$, $d(c_{a0}) = -1$)	Indicates that the measured parameter increases or decreases directly with a desired or not desired biological effect.
$f(v_{ij})_{\text{obs}}$	=IF(AND($v_{ij} > \text{cutoff}(c_{a0})$, $d(c_{a0}) = 1$), 1, IF(AND($v_{ij} \leq \text{cutoff}(c_{a0})$, $d(c_{a0}) = -1$), 1, 0))	$f(v_{ij})_{\text{obs}} = 1$ for active compounds or $f(v_{ij})_{\text{obs}} = 0$ for control group according to the set of cutoff and desirability values used for each c_{a0} . It is the function used as output to train the IFPTML model.
$n(f(v_{ij}) = 1)$	=COUNTIF(Range(c_{a0}), Criteria(c_{a0}), Range($f(v_{ij})_{\text{obs}}, 1$))	Function that determines the total number of each Biological activity in the dataset and $f(v_{ij})_{\text{obs}}$ equal to 1.
$f(v_{ij})_{\text{ref}}$	= $n(f(v_{ij}) = 1) / n_j(c_{a0})$	The function of reference $f(v_{ij})_{\text{ref}} = p(f(v_{ij}) = 1 / c_{a0})$ is the probability with which the observed function gets the value $f(v_{ij})_{\text{obs}} = 1$, positive assay. It is used as the first input variable of the IFPTML model.

4.8. Shannon Entropy Measures

The previous IFPTML equations were inputted as $\text{Sh}(\text{Subsystem}_s)_k$ variables. We calculated the Shannon's Entropies values $\text{Sh}(\text{Drug})_k$, $\text{Sh}(\text{Prot})_k$, $\text{Sh}(\text{Gene})_k$, and $\text{Sh}(\text{Chrom})_k$ to quantify the structure information of the different subsystems. We used the tool MARKovCHains Invariants for Network Selection and DEsign (MARCH-INSIDE) to calculate the $\text{Sh}(\text{Drug})_k$ values of drugs [48]. The software MARCH-INSIDE was used to input the Simplified Molecular Input Line Entry Specification (SMILES) codes for each compound downloaded from ChEMBL. On the other hand, we used the tool Sequences to Networks (S2SNet) [28] to calculate information index values $\text{Sh}(\text{Prot})_k$, $\text{Sh}(\text{Gene})_k$, and $\text{Sh}(\text{Chrom})_k$ about the sequence and recurrence of different amino acids into the proteins, nucleotides into the genes, and genes into the chromosomes. The software S2SNet was used to input the sequences of proteins and genes downloaded from UniProt and NCBI-GDV, respectively. S2SNet was also used to input a np (negative/positive) sequence code to express the orientation of reading and position of each gene into the chromosome.

Both MARCH-INSIDE (drugs) and S2SNet (proteins, genes, and chromosomes) use a graph to represent the parts of the subsystem (nodes) and the relationships (link) among them into the structure of the subsystem. The parts of the subsystems are atoms, amino acids, nucleotide bases, or genes. The links among them are chemical bonds, peptide bonds, gene sequence, or gene position according to the system. The S2SNet software also takes into account relationships of recurrence to specific types of amino acids, nucleotides,

and gene orientation. Figure 7 illustrates some examples of the graphs used to represent the different subsystems. It shows the name, the representation graph, and a small part of the graph with its nodes and links. We can see in this figure, from bottom to top, the chromosome XI represented by genes and the links to the pairs of genes with inverse orientation. The graph's nodes of gene 285 with its representation graph in the chromosome, and the graph with its nodes represented by the nucleotides and links represented by the gene sequence by their recurrences. The protein Q9NFSS has nodes to amino acids and links to peptide bonds and the recurrence. Finally, the graph of the CHEMBL510738 drug was represented with atoms (nodes) and Chemical Bonds (links).

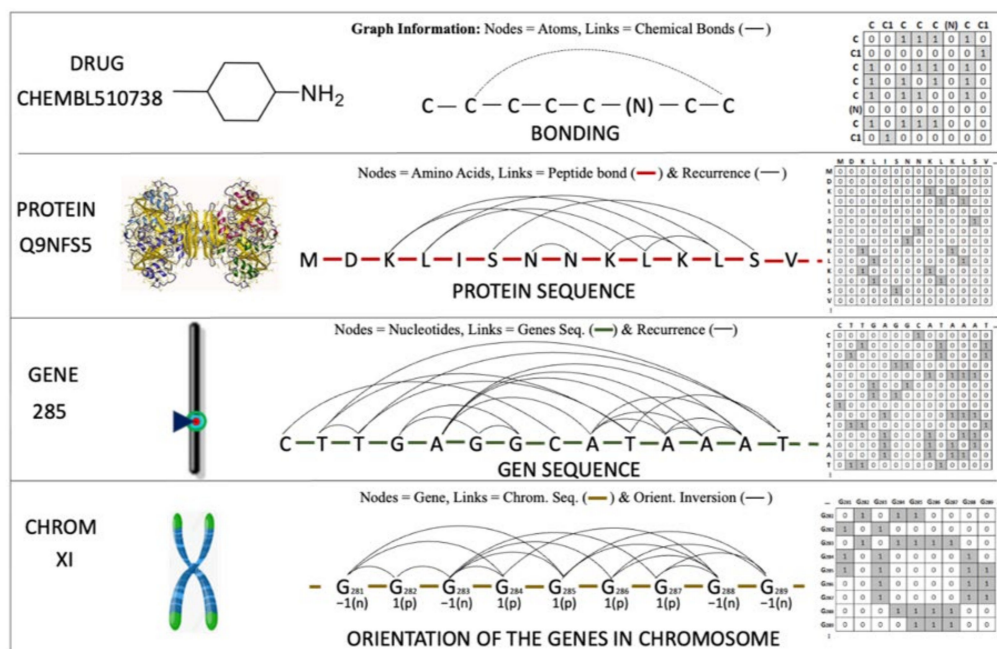


Figure 7. Illustration of different representations to represent multiple molecular systems.

Both MARCH-INSIDE and S2SNet associates a node adjacency matrix $A(\text{Subsystem}_s)$ to the respective graphs to carry out a numerical representation of the system (see Figure 7). Next, both software transforms the adjacency matrix of each subsystem $A(\text{Subsystem}_s)$ into a Markov matrix $\Pi_1(\text{Subsystem}_s)$, not represented in Figure 7. After that, both tools calculate the natural powers of order k^{th} for each matrix $\Pi_1(\text{Subsystem}_s)$. Last, both software use the Chapman-Kolmogórov equations to calculate the absolute probabilities ${}^a p(n/s)_k$ for each node in a given subsystem (n/s) [28,48]. With these probabilities and the Equation (5), the software performs the calculation of the different $\text{Sh}(\text{Drug})_k$, $\text{Sh}(\text{Prot})_k$, $\text{Sh}(\text{Gene})_k$, and $\text{Sh}(\text{Chrom})_k$ values.

$$\text{Sh}(\text{Subsystem}_s)_k = - \sum_{n=1}^{n_{\max}} {}^a p(n, s)_k \cdot \log({}^a p(n, s)_k) \quad (5)$$

4.9. Partitions of Categorical Variables

We created two partitions (subsets) of categorical variables from ChEMBL dataset to encode all the functional or non-structural information. The first partition of categorical variables was $c_{\text{assay}j}$ (abbreviated as c_{aj}). The second partition was $c_{\text{data}j}$ (abbreviated as c_{dj}). These partitions contain variables that encode information about experimental conditions of preclinical assays (c_{aj}) or about the nature and quality of data (c_{dj}). These categorical variables include information about 22 biological activity types (c_{a0}), 28 target proteins (c_{a1}), and 9 organisms of the assay (c_{a2}), etc. We also created another partition ($c_{\text{prot}j} = c_{pj}$) including categorical variables with biological information about the target proteins, genes,

and chromosomes. These variables cover 32 genes (c_{p0}), 10 chromosomes (c_{p1}), gene orientation (c_{p2}), and 31 protein functions (c_{p3}). Table 7 depicts details of these partitions.

Table 7. Partitions and levels (unique values) taken by the categorical (not ordered) input variables.

Partition (c_j)	Var.	Information	NL ^a	Unique Levels
c_{assayj} (c_{aj})	c_{a0}	Biological activity	22	Inhibition(%); IC ₅₀ (nM); K _i (nM); IC ₅₀ (ug.mL ⁻¹); BHIA ₅₀ (-); IC ₅₀ (mill equivalent); FC(-); K _{inact} (/min); Activity(%); VAR(-); Ratio(-); Ratio(/M/s); IC ₅₀ (molar ratio); Ratio IC ₅₀ (-); Mean(pM mg ⁻¹); GST activity (mU mg ⁻¹); K _m (nM); Ratio(/s/M); Activity(-); K _a (10 ³ /M/s); K _{cat} (/s); Inhibition(uM)
	c_{a1}	UniProt protein accession ID	28	Q8MU52; Q3HTL5; Q9NBA7; Q9NFS5; Q8T6J6; Q25856; P39898; Q9N6S8; Q0PJ46; Q6T755; Q8MMZ4; Q868D6; Q25917; Q9GSW0; Q9NAW4; O77078; Q9NAW2; Q9BJJ9; Q8T6B1; Q9N623; Q9XYC7; P05227; P11144; Q17SB2; O77239; Q9Y006; O96214; O97467
	c_{a2}	Assay Organism	9	<i>Plasmodium falciparum</i> ; <i>Plasmodium falciparum</i> K1; <i>Plasmodium falciparum</i> NF54; <i>Plasmodium falciparum</i> Dd2; <i>Plasmodium</i> sp.; <i>Plasmodium yoelii</i> ; <i>Plasmodium berghei</i> ; <i>Leishmania Mexicana</i> ; ND (No registered data)
c_{dataj} (c_{dj})	c_{d0}	Target mapping	2	Protein; Homologous protein
	c_{d1}	APD name	9	Peptidase C1; Pkinase; Peptidase S8; Asp; OMPdecase; Spermine synth; Sugar tr; Hist deacetyl
	c_{d2}	APD confidence	2	ND (No-Data); high
	c_{d3}	Assay type	2	Binding (B) = Data measuring binding of compound to a molecular target. Functional (F) = Data measuring the biological effect of a compound.
	c_{d4}	Data curation level	3	Autocuration; Intermediate; Expert
	c_{d5}	Confidence score	2	8 = Homologous single protein target assigned. 9 = Direct single protein target assigned
c_{p0}	Gene	32	PF140187; PF110161; PFB0325c; PF110301; PF100225; PF140341; PF140075; PF110165; PF130141; MAL13P1.214; PF140346; PFE0355c; PF140294; PF140125; PF110162; PFB0505c; PF140511; PF140076; PFE0370c; PF110147; PFB0330c; PFF0730c; PF140598; MAL7P1.27; PFI1260c; PFB0100c; PF080054; PF140077; MAL13P1.185; PF140078; PFB0150c; PFE1455w	
c_{p1}	Chromosome	10	II; V; VI; VII; VIII; IX; X; XI; XIII; XIV	
c_{p2}	Orientation	2	Downstream = -1; Upstream = 1	
c_{protj} (c_{pj})	c_{p3}	Protein function (UniProt)	31	Glutathione s-transferase, putative; Falcipain-2 precursor; Cysteine protease, putative; Spermidine synthase; Orotidine-monophosphate-decarboxylase, putative; Glucose-6-phosphate isomerase; Plasmepsin, putative; Falcipain 2 precursor; L-lactate dehydrogenase; phosphoethanolamineN-methyltransferase; cGMP-dependent protein kinase 1, beta isozyme, putative; Serine protease belonging to subtilisin family, putative; Mitogen-activated protein kinase 1; Deoxyhypusine synthase; Falcipain-3; Beta-ketoacyl-acyl carrier protein synthase III precursor, putative; Glucose-6-phosphate dehydrogenase-6-phosphogluconolactonase; Plasmepsin 1 precursor; Subtilisin-like protease precursor, putative; Mitogen-activated protein kinase 2; Enoyl-acyl carrier reductase; Glyceraldehyde-3-phosphate dehydrogenase; Chloroquine resistance transporter, putative; Histone deacetylase; Knob associated histidine-rich protein; Heat shock 70 kDa protein; Plasmepsin 2 precursor; CDK-related protein kinase 6; HAP protein; Protein kinase, putative; Sugar transporter, putative
	c_{p4}	ChEMBL target function type	5	Enzyme; Transporter; Epigenetic regulator; Other cytosolic protein; Unclassified Protein

^a NL = Number of Levels (unique values) remaining after pre-processing.

4.10. Perturbation-Theory Operators (PTOs)

As we mentioned before, the IFPTML model use PTOs to quantify the deviation (perturbations) in continuous variables (structural parameters, time, concentration, etc.) with respect to functional information encoded by categorical variables c_j (experimental conditions). In this work we selected the MMAs operators of type PTO($\text{Sh}(\text{Subsystem}_s)_k$) $= \Delta\text{Sh}(\text{Subsystem}_s)_{k,c_j} = \text{Sh}(\text{Subsystem}_1)_k - \langle \text{Sh}(\text{Subsystem}_1)_{k,c_j} \rangle$ or $f(\text{Sh}(\text{Subsystem}_s)_k) = \Delta\text{Sh}(\text{Subsystem}_s)_{k,c_j} = \text{Sh}(\text{Subsystem}_1)_k - \langle \text{Sh}(\text{Subsystem}_1)_{k,c_j} \rangle$. These operators quantify the deviation (gain or loss in information) of the specific value $\text{Sh}(\text{Subsystem}_1)_k$ of the subsystem concerning the average $\langle \text{Sh}(\text{Subsystem}_1)_{k,c_j} \rangle$ (expected value) of information for all cases measured under the same experimental conditions. We used three different partitions c_j of categorical variables to codify the experimental conditions and/or non-structural information (see next section). Moreover, in this data pre-processing stage, we have calculated the PT operators similar to Box-Jenkins MA operators that are used as input data. In this context, c (with c in boldface) refers to a vector of multiple combinations of categorical variables at the same time. The partitions of the categorical variables used here are c_{assayj} , c_{protj} , and c_{dataj} . These partitions are fusions of categorical variables related to the pharmacological assay (c_{assayj}), the nature of the drug target (c_{protj}), or about the nature and/or accuracy of the data measured (c_{dataj}). For simplicity's sake, we abbreviate these partitions as $c_{\text{assayj}} = c_{aj}$, $c_{\text{protj}} = c_{pj}$, and $c_{\text{dataj}} = c_{dj}$. The partition $c_{aj} = (c_{a0}, c_{a1}, c_{a2})$ included the following categorical variables: biological activity (c_{a0}), the UniProt protein accession ID (c_{a1}), and the organism of assay (c_{a2}). In the Supplementary Materials we detailed all fused datasets of drugs, unique sequences, proteins, chromosomes, genes, Shannon Entropies values, and the PTO's values, this process is called the IF technique. Table 8 shows details of the Perturbation-Theory Operators.

Table 8. Input variables of the IFPTML models developed.

Variable Type	Symbol	Formula	Categorical Variables	Details
-	$f(v_{ij})_{\text{ref}}$	$n(f(v_{ij})_{\text{expt}} = 1)/n_j$	c_{a0}	Expected value of probability $p(f(v_{ij}) = 1)_{\text{ref}}$ for the activity v_{ij} of type c_{a0} .
$\text{MMA}_{c_{aj}}$	$\Delta\text{Sh}(\text{Drug}_i)_{k,c_{aj}}$	$\text{Sh}(\text{Drug}_i)_k - \langle \text{Sh}(\text{Drug})_{k,c_{aj}} \rangle$	c_{aj}	Variation (Δ) of the information of the structure of the drug in different subsets of multiple categorical variables related to the pharmacological assay c_{aj} .
$\text{MMA}_{c_{dj}}$	$\Delta\text{Sh}(\text{Drug}_i)_{k,c_{dj}}$	$\text{Sh}(\text{Drug}_i)_k - \langle \text{Sh}(\text{Drug})_{k,c_{dj}} \rangle$	c_{dj}	Variation (Δ) of the information of the structure of the drug in different subsets of multiple categorical variables related to the nature and/or accuracy of the data measured c_{dj} .
$\text{MMA}_{c_{pj}}$	$\Delta\text{Sh}(\text{Prot}_i)_{k,c_{pj}}$	$\text{Sh}(\text{Prot}_i)_k - \langle \text{Sh}(\text{Prot})_{k,c_{pj}} \rangle$	c_{pj}	Variation (Δ) of the information of the sequence of the protein, sequence of the gene, and information about the chromosome for different subsets of multiple categorical variables related to the nature of the protein target c_{pj} .
	$\Delta\text{Sh}(\text{Gene}_i)_{k,c_{pj}}$	$\text{Sh}(\text{Gene}_i)_k - \langle \text{Sh}(\text{Gene})_{k,c_{pj}} \rangle$		
	$\Delta\text{Sh}(\text{Chrom}_i)_{k,c_{pj}}$	$\text{Sh}(\text{Chrom}_i)_k - \langle \text{Sh}(\text{Chrom})_{k,c_{pj}} \rangle$		

4.11. IFPTML Model Training and Validation

The first step to develop the IFPTML models [12–17] was to download all the information about preclinical assays, drugs structure, protein sequences, gene sequences, and chromosomes information from public databases (ChEMBL, UniProt, NCBI-GDV). The second step was to carry out a pre-processing of all the previous information in order to calculate the $f(v_{ij})_{\text{obs}}$ (dependent variable) and $f(v_{ij})_{\text{ref}}$. Next, we calculated the

Sh(Subsystem_s)_k values (input variables). This includes a process of information fusion including data from the different databases (ChEMBL, UniProt, NCBI-GDV). Once data have been prepared for analysis, we then run the ML algorithms General Discriminant Analysis (GDA), Classification Tree (CT) with Univariate Splits (CTUS), and CT with Linear Combination (CTLC) to seek alternative IFPTML models. All the IFPTML models were developed using STATISTICA [30] software v. 12.

5. Conclusions

Computational prediction of new Antimalarial compounds is a very important goal for the pharmaceutical industry. However, the huge amount of information available from different sources makes the analysis of data for the discovery of new compounds difficult. The IFPTML method allowed us to conduct the fusion and analysis of three different datasets from the databases ChEMBL, UniProt, and NCBI-GDV to achieve this goal. The ChEMBL dataset contains outcomes for 17,758 unique assays including numeric descriptors (variables) for the structure of compounds. The IFPTML algorithm was successful in accounting for both numerical information (structural parameters) and categorical information (multiple experimental conditions) of the three datasets. Shannon's entropy measures Sh_k (numerical variables) were useful to quantify the information about the structure of drugs, protein sequences, gene sequences, and chromosomes. In addition, MMAs of different partitions of categorical variables from categorical variables from the ChEMBL dataset were useful to encode multiple experimental conditions of preclinical assays and information about targets proteins, genes, and chromosomes. The IFPTML-CTLC model is the most complex in terms of number of input variables, number of LCs, and number of splitting rules. However, the IFPTML-CTLC model showed better performance than the IFPTML-GDA and includes more biologically relevant information than the IFPTML-CTUS model. This model could become a useful tool for the optimization of pre-clinical assays of new Antimalarial compounds taking into consideration the structure of the drug, the specie of *Plasmodium*, the sequence of the target protein, and other multiple parameters.

Supplementary Materials: The following are available online at <https://www.mdpi.com/article/10.3390/ijms222313066/s1>.

Author Contributions: Conceptualization, H.G.-D. and V.Q.-T.; methodology, H.G.-D., V.Q.-T. and B.O.-T.; software, B.O.-T.; validation, H.G.-D. and V.Q.-T.; formal analysis, H.G.-D. and V.Q.-T.; investigation, H.G.-D. and V.Q.-T.; resources, H.G.-D.; data curation, H.G.-D. and V.Q.-T.; writing—original draft preparation H.G.-D. and V.Q.-T.; writing—review and editing, H.G.-D., V.Q.-T. and B.O.-T.; visualization, H.G.-D. and V.Q.-T., H.G.-D.; project administration, H.G.-D.; funding acquisition, H.G.-D. and V.Q.-T. All authors have read and agreed to the published version of the manuscript.

Funding: H.G.-D. personally acknowledges financial support from the Minister of Science and Innovation (PID2019-104148GB-I00) and a grant (IT1045-16)—2016–2021 from the Basque Government. V.Q.T. acknowledges Universidad Estatal Amazónica (UEA) scholarship for postgraduate studies; Ecuador Sciences PhD Program, (UEA.Res.26.2019.06.13).

Institutional Review Board Statement: Not applicable.

Informed Consent Statement: Not applicable.

Data Availability Statement: Data supporting the reported results can be found in the Supplementary Materials file.

Conflicts of Interest: The authors declare no conflict of interest.

References

1. Alonso, P.; Noor, A.M. The global fight against malaria is at crossroads. *Lancet* **2017**, *390*, 2532–2534. [CrossRef]
2. Kalanon, M.; McFadden, G.I. Malaria, *Plasmodium falciparum* and its apicoplast. *Biochem. Soc. Trans.* **2010**, *38*, 775–782. [CrossRef]

3. Gaillard, T.; Boxberger, M.; Madamet, M.; Pradines, B. Has doxycycline, in combination with anti-malarial drugs, a role to play in intermittent preventive treatment of *Plasmodium falciparum* malaria infection in pregnant women in Africa? *Malar. J.* **2018**, *17*, 469. [[CrossRef](#)]
4. DiMasi, J.A.; Grabowski, H.G.; Hansen, R.W. Innovation in the pharmaceutical industry: New estimates of R&D costs. *J. Health Econ.* **2016**, *47*, 20–33.
5. Gaulton, A.; Hersey, A.; Nowotka, M.; Bento, A.P.; Chambers, J.; Mendez, D.; Mutowo, P.; Atkinson, F.; Bellis, L.J.; Cibrian-Uhalte, E.; et al. The ChEMBL database in 2017. *Nucleic Acids Res.* **2017**, *45*, D945–D954. [[CrossRef](#)]
6. Gaulton, A.; Bellis, L.J.; Bento, A.P.; Chambers, J.; Davies, M.; Hersey, A.; Light, Y.; McGlinchey, S.; Michalovich, D.; Al-Lazikani, B.; et al. ChEMBL: A large-scale bioactivity database for drug discovery. *Nucleic Acids Res.* **2012**, *40*, D1100–D1107. [[CrossRef](#)]
7. Wolfsberg, T.G. Using the NCBI map viewer to browse genomic sequence data. *Curr. Protoc. Bioinform.* **2010**, *29*, 1–5. [[CrossRef](#)] [[PubMed](#)]
8. Coordinators, N.R. Database resources of the National Center for Biotechnology Information. *Nucleic Acids Res.* **2018**, *46*, D13–D21. [[CrossRef](#)]
9. UniProt Consortium. UniProt: A worldwide hub of protein knowledge. *Nucleic Acids Res.* **2019**, *47*, D506–D515. [[CrossRef](#)] [[PubMed](#)]
10. UniProt Consortium. UniProt: The universal protein knowledgebase. *Nucleic Acids Res.* **2018**, *46*, 2699. [[CrossRef](#)] [[PubMed](#)]
11. Pundir, S.; Martin, M.J.; O'Donovan, C. UniProt Protein Knowledgebase. *Methods Mol. Biol.* **2017**, *1558*, 41–55.
12. Gonzalez-Diaz, H.; Arrasate, S.; Gomez-SanJuan, A.; Sotomayor, N.; Lete, E.; Besada-Porto, L.; Ruso, J.M. General theory for multiple input-output perturbations in complex molecular systems. 1. linear QSPR electronegativity models in physical, organic, and medicinal chemistry. *Curr. Top. Med. Chem.* **2013**, *13*, 1713–1741. [[CrossRef](#)] [[PubMed](#)]
13. Santana, R.; Zuluaga, R.; Gañán, P.; Arrasate, S.; Onieva, E.; González-Díaz, H. Designing nanoparticle release systems for drug-vitamin cancer co-therapy with multiplicative perturbation-theory machine learning (PTML) models. *Nanoscale* **2019**, *11*, 21811–21823. [[CrossRef](#)] [[PubMed](#)]
14. Nocado-Mena, D.; Cornelio, C.; Camacho-Corona, M.D.R.; Garza-Gonzalez, E.; Waksman de Torres, N.; Arrasate, S.; Sotomayor, N.; Lete, E.; Gonzalez-Diaz, H. Modeling antibacterial activity with machine learning and fusion of chemical structure information with microorganism metabolic networks. *J. Chem. Inf. Model.* **2019**, *59*, 1109–1120. [[CrossRef](#)] [[PubMed](#)]
15. Shannon, C.E. A Mathematical theory of communication. *Bell Syst. Tech. J.* **1948**, *27*, 379–423. [[CrossRef](#)]
16. Graham, D.J. Information content in organic molecules: Structure considerations based on integer statistics. *J. Chem. Inf. Comput. Sci.* **2002**, *42*, 215. [[CrossRef](#)]
17. Graham, D.J.; Malarkey, C.; Schulmerich, M.V. Information content in organic molecules: Quantification and statistical structure via brownian processing. *J. Chem. Inf. Comput. Sci.* **2004**, *44*, 1601–1611. [[CrossRef](#)]
18. Graham, D.J.; Schacht, D. Base Information content in organic molecular formulae. *J. Chem. Inf. Comput. Sci.* **2000**, *40*, 942. [[CrossRef](#)]
19. Graham, D.J.; Schulmerich, M.V. Information content in organic molecules: Reaction pathway analysis via brownian processing. *J. Chem. Inf. Comput. Sci.* **2004**, *44*, 1612–1622. [[CrossRef](#)] [[PubMed](#)]
20. Graham, D.J. Information content and organic molecules: Aggregation states and solvent effects. *J. Chem. Inf. Model.* **2005**, *45*, 1223–1236. [[CrossRef](#)]
21. Graham, D.J. Information content in organic molecules: Brownian processing at low levels. *J. Chem. Inf. Model.* **2007**, *47*, 376–389. [[CrossRef](#)] [[PubMed](#)]
22. Contreras-Torres, E.; Marrero-Ponce, Y.; Teran, J.E.; Garcia-Jacas, C.R.; Brizuela, C.A.; Sanchez-Rodriguez, J.C. MuLiMs-MCoMPAs: A novel multiplatform framework to compute tensor algebra-based three-dimensional protein descriptors. *J. Chem. Inf. Model.* **2019**, *60*, 1042–1059. [[CrossRef](#)] [[PubMed](#)]
23. Martinez-Lopez, Y.; Marrero-Ponce, Y.; Barigye, S.J.; Teran, E.; Martinez-Santiago, O.; Zambrano, C.H.; Torres, F.J. When global and local molecular descriptors are more than the sum of its parts: Simple, but not simpler? *Mol. Divers.* **2019**, *24*, 913–932. [[CrossRef](#)]
24. Valdes-Martini, J.R.; Marrero-Ponce, Y.; Garcia-Jacas, C.R.; Martinez-Mayorga, K.; Barigye, S.J.; Vazd'Almeida, Y.S.; Pham-The, H.; Perez-Gimenez, F.; Morell, C.A. QuBiLS-MAS, open source multi-platform software for atom- and bond-based topological (2D) and chiral (2.5D) algebraic molecular descriptors computations. *J. Cheminform.* **2017**, *9*, 35. [[CrossRef](#)]
25. Ruiz-Blanco, Y.B.; Paz, W.; Green, J.; Marrero-Ponce, Y. ProtDCal: A program to compute general-purpose-numerical descriptors for sequences and 3D-structures of proteins. *BMC Bioinform.* **2015**, *16*, 162. [[CrossRef](#)]
26. Ruiz-Blanco, Y.B.; Marrero-Ponce, Y.; Paz, W.; Garcia, Y.; Salgado, J. Global stability of protein folding from an empirical free energy function. *J. Theor. Biol.* **2013**, *321*, 44–53. [[CrossRef](#)]
27. Barigye, S.J.; Marrero-Ponce, Y.; Martinez-Lopez, Y.; Torrens, F.; Artilles-Martinez, L.M.; Pino-Urias, R.W.; Martinez-Santiago, O. Relations frequency hypermatrices in mutual, conditional and joint entropy-based information indices. *J. Comput. Chem.* **2013**, *34*, 259–274. [[CrossRef](#)]
28. Munteanu, C.R.; Gonzalez-Diaz, H.; Borges, F.; de Magalhaes, A.L. Natural/random protein classification models based on star network topological indices. *J. Theor. Biol.* **2008**, *254*, 775–783. [[CrossRef](#)]

29. Quevedo-Tumaili, V.F.; Ortega-Tenezaca, B.; Gonzalez-Diaz, H. Chromosome gene orientation inversion networks (GOINs) of plasmodium proteome. *J. Proteome Res.* **2018**, *17*, 1258–1268. [[CrossRef](#)] [[PubMed](#)]
30. Mendez, D.; Gaulton, A.; Bento, A.P.; Chambers, J.; De Veij, M.; Félix, E.; Magarinos, M.P.; Mosquera, J.F.; Mutowo, P.; Nowotka, M.; et al. ChEMBL: Towards direct deposition of bioassay data. *Nucleic Acids Res.* **2019**, *47*, D930–D940. [[CrossRef](#)]
31. Nowotka, M.M.; Gaulton, A.; Mendez, D.; Bento, A.P.; Hersey, A.; Leach, A. Using ChEMBL web services for building applications and data processing workflows relevant to drug discovery. *Expert Opin. Drug. Discov.* **2017**, *12*, 757–767. [[PubMed](#)]
32. Davies, M.; Nowotka, M.; Papadatos, G.; Dedman, N.; Gaulton, A.; Atkinson, F.; Bellis, L.; Overington, J.P. ChEMBL web services: Streamlining access to drug discovery data and utilities. *Nucleic Acids Res.* **2015**, *43*, W612–W620. [[CrossRef](#)]
33. Bento, A.P.; Gaulton, A.; Hersey, A.; Bellis, L.J.; Chambers, J.; Davies, M.; Kruger, F.A.; Light, Y.; Mak, L.; McGlinchey, S.; et al. The ChEMBL bioactivity database: An update. *Nucleic Acids Res.* **2014**, *42*, D1083–D1090. [[CrossRef](#)]
34. Sastry, G.M.; Inakollu, V.S.; Sherman, W. Boosting virtual screening enrichments with data fusion: Coalescing hits from two-dimensional fingerprints, shape, and docking. *J. Chem. Inf. Model.* **2013**, *53*, 1531–1542. [[CrossRef](#)]
35. Willett, P. Combination of similarity rankings using data fusion. *J. Chem. Inf. Model.* **2013**, *53*, 1–10. [[CrossRef](#)]
36. Whittle, M.; Gillet, V.J.; Willett, P.; Loesel, J. Analysis of data fusion methods in virtual screening: Similarity and group fusion. *J. Chem. Inf. Model.* **2006**, *46*, 2206–2219. [[CrossRef](#)]
37. Whittle, M.; Gillet, V.J.; Willett, P.; Loesel, J. Analysis of data fusion methods in virtual screening: Theoretical model. *J. Chem. Inf. Model.* **2006**, *46*, 2193–2205. [[CrossRef](#)] [[PubMed](#)]
38. Weininger, D. SMILES, a chemical language and information system. 1. Introduction to methodology and encoding rules. *J. Chem. Inf. Model.* **1988**, *28*, 31–36. [[CrossRef](#)]
39. Toropov, A.A.; Benfenati, E. SMILES as an alternative to the graph in QSAR modelling of bee toxicity. *Comput. Biol. Chem.* **2007**, *31*, 57–60. [[CrossRef](#)] [[PubMed](#)]
40. Veselinovic, A.M.; Milosavljevic, J.B.; Toropov, A.A.; Nikolic, G.M. SMILES-based QSAR model for arylpiperazines as high-affinity 5-HT(1A) receptor ligands using CORAL. *Eur. J. Pharm. Sci.* **2013**, *48*, 532–541. [[CrossRef](#)] [[PubMed](#)]
41. Leone, C.; Bertuzzi, E.E.; Toropova, A.P.; Toropov, A.A.; Benfenati, E. CORAL: Predictive models for cytotoxicity of functionalized nanozeolites based on quasi-SMILES. *Chemosphere* **2018**, *210*, 52–56. [[CrossRef](#)]
42. Pogany, P.; Arad, N.; Genway, S.; Pickett, S.D. De novo molecule design by translating from reduced graphs to SMILES. *J. Chem. Inf. Model.* **2019**, *59*, 1136–1146. [[CrossRef](#)] [[PubMed](#)]
43. Toropova, A.P.; Toropov, A.A. Quasi-SMILES: Quantitative structure-activity relationships to predict anticancer activity. *Mol. Divers.* **2019**, *23*, 403–412. [[CrossRef](#)]
44. Zheng, S.; Yan, X.; Yang, Y.; Xu, J. Identifying structure-property relationships through SMILES syntax analysis with self-attention mechanism. *J. Chem. Inf. Model.* **2019**, *59*, 914–923. [[CrossRef](#)]
45. Prado-Prado, F.; García-Mera, X.; Abeijón, P.; Alonso, N.; Caamaño, O.; Yáñez, M.; Gárate, T.; Mezo, M.; González-Warleta, M.; Muiño, L.; et al. Using entropy of drug and protein graphs to predict FDA drug-target network: Theoretic-experimental study of MAO inhibitors and hemoglobin peptides from *Fasciola hepatica*. *Eur. J. Med. Chem.* **2011**, *46*, 1074–1094. [[CrossRef](#)] [[PubMed](#)]
46. Hill, T.; Lewicki, P. *STATISTICS Methods and Applications. A Comprehensive Reference for Science, Industry and Data Mining*; StatSoft: Tulsa, OK, USA, 2006; Volume 1, p. 813.
47. Tilley, L.; Rosenthal, P.J. Malaria parasites fine-tune mutations to resist drugs. *Nature* **2019**, *576*, 217–219. [[CrossRef](#)]
48. Zhao, L.; Pi, L.; Qin, Y.; Lu, Y.; Zeng, W.; Xiang, Z.; Qin, P.; Chen, X.; Li, C.; Zhang, Y.; et al. Widespread resistance mutations to sulfadoxine-pyrimethamine in malaria parasites imported to China from Central and Western Africa. *Int. J. Parasitol. Drugs Drug Resist.* **2019**, *12*, 1–6. [[CrossRef](#)] [[PubMed](#)]